Biomacromol. J., Vol. 8, No. 1, 25-34, July 2022.

Biomacromolecular Journal
www.bmmj.org

Synthesis, Characterization and Cytotoxicity Activities of Iron Oxide Nanoparticles and Pegylated Iron Oxide Nanoparticles Using the *Zhumeria Majdae* Indigenous to South Iran (Hormozgan)

M. Poodat[a], A. Divsalar[b,*], B. Ghalandari[c,d] and R. Khavarinezhad[a]

[a]*Department of Biology, Science and Research Branch, Islamic Azad University, Tehran, Iran*

[b]*Department of Cell & Molecular Biology, Faculty of Biological Sciences, Kharazmi University, Tehran, Iran*

[c]*Department of Medical Nanotechnology, Applied Biophotonics Research Center, Science and Research Branch, Islamic Azad University, Tehran, Iran*

[d]*Current Address: State Key Laboratory of Oncogenes and Related Genes, Institute for Personalized Medicine, School of Biomedical Engineering, Shanghai Jiao Tong University, Shanghai, China*

(Received 15 January 2023, Accepted 30 January 2023)

ABSTRACT

Nanotechnology has been researched over the past decades for green synthesis of iron oxide nanoparticles (IONPs); revealing the significance of plant extracts in reducing the iron precursor salt to nanoparticles and their applications in various domains. *Zhumeria majdae (*Mohre-khosh) is an aromatic herb, belonging to the family Lamiaceae that grows wild just in Hormozgan Province, southern Iran. It has reported that the leaves of *Zhumeria majdae* contain phytocompounds like flavonoids, diterpenoids and triterpenes. Herein, the leaves of *Zhumeria majdae* are used for the first time as a reducing agent. Present work emphasized on the synthesis of iron oxide nanoparticles using *Zhumeria majdae* leaves for targeted drug delivery for breast cancer. IONPs were characterized and their Cytotoxicity effects were srudied on the breast cancer cell line MCF-7 and Human embryonic kidney (Hek293). The use of the metabolic extract of *Zhumeria majdae* leaf indicated the involvement of phytocompounds in reducing the iron oxides and capping and stabilizing their nanoparticles. Finally, cytotoxicity assay revealed that the obtained IONPs have potential cytotoxicity against breast cancer cell line of MCF-7.

Keywords: Iron oxide nanoparticles, Zhumeria majdae, Metabolic extract, Cytotoxicity

INTRODUCTION

Recently, biosynthesized magnetic nanoparticles, especially magnetite iron oxide nanoparticles (IONPs), have found wide applications in the biomedical field [1]. IONPs can be synthesized through Physical and chemical methods such as chemical precipitation, sol-gel, mineralization flow injection, microemulsion, hydrothermal, hydrolysis and electrochemical technique [2]. these methods have had several limitations, including high production costs, toxic chemical species and the production of hazardous by products [3]. Plant-based nanoparticles synthesis has advantages, such as biocompatibility, producing less waste, free availability of plants, nontoxic, cost effectiveness, easily conjugation with metal oxide- based nanoparticles to produce targeted drug delivery systems [4,5]. It is reported that the Plant products/extracts-mediated nanoparticles are more stable and the rate of synthesis easy when compared with the traditional synthesis techniques [6]. Also, phytochemicals present in the extract prevent the agglomeration of the nanoparticles by forming monolayer around the nanoparticles. It strongly affects size distribution of nanoparticles; resulting in the synthesis of nanoparticles with smaller size and narrow size distribution [7]. Zhumeria majdae, a popular medicinal herb growing exclusively in Hormozgan province (South of Iran), Therapeutic properties have been previously proven for the Zhumeria majdae, namely anti-inflammatory, anti-nociceptive, anti-microbial, anti-diabetic, herpes simplex type 1 inhibitory, anti-leishmanial, anti-plasmodial, repellent, anti-cancer, anti-

*Corresponding author. E-mail: divsalar@khu.ac.ir

oxidant, anti-malaria, anti-seizure,acetylcholinesterase inhibitory and α- glucosidase inhibitory activities [8,9]. Because of its high bioactive and antioxidant compounds, such as polyphenols [10] that provides an excelent reducing and capping agent for nanoparticles synthesis. Regarding anti-cancer properties, Zhumeria majdae is Capable of killing various cancer cells [11]. This study aims to develop an appropriate protocol for biosynthesis and characterization of iron oxide nanoparticles using Z.majdae leaves, given the drug delivery applications. The green synthesized Zhumeria majdae/nanoparticles were characterized by UV-Vis spectroscopy, Dynamic light scattering (DLS), Zeta potential, Fourier transform-Infrared spectroscopy (FT-IR), X-ray diffraction (XRD), field emission scanning electron microscope (FE-SEM), Atomic force microscop (AFM) and vibration sample magnetometer (VSM) analysis. Finally, the synthesized Zhumeria majdae/nanoparticles have been studied for their anticancer activity. The schematic of the nanoparticle synthesis process is shown in Fig. 1.

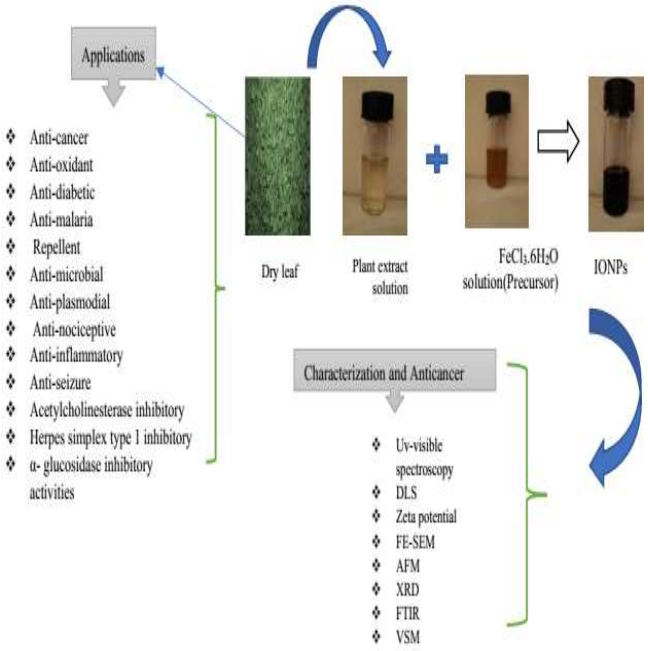

Fig. 1. Schematic of the synthesis process for iron oxide nanoparticles using Zhumeria majdae leaves extract.

MATERIAL AND METHODS

Chemical, Rreagents and Sample Collection

The *Zhumeria majdae* leaves were collected from the Genow region of Hormozgan, Iran. Iron chloride hexahydrate was obtained from Sigma-Aldrich. Methanol was used for extraction. polyethylene $glycol_{4000}$, was prepared from chemical supplier (Sigma-Aldrich).

Preparation of Zhumeria Majdae Leaf Extract

The *Zhumeria majdae* leaves were washed with deionized water and then, 50 g leaf was ground in an electrical grinder and mixed with 400 ml of methanol and shaken at 180 rpm at 37 °C for 48 h. The extract was stored at 4 °C and used for the preparation of IONPs.

Pegylated-iron Oxide Nanoparticles Synthesis Procedure

The extract and iron chloride solution (1 M) were mixed in 1:2 ratio. The mixture was heated in an incubator shaker at 45 °C for 8 h and 180 rpm. Then, it was centrifuged at 15,000 rpm for 20 min and 4 °C. Sediments was washed with deionized water and ethanol (3 times) and was dried for 24 h in oven at 40 °C and used for further uses. 20 mg of particles were stirred with 10 ml of 80 mM PEG solution for 12 h at ambient temperature. The solution was centrifuged twice at 3200 rpm for ten minutes and was washed with deionized water. The resulting Sediments was then washed with ethanol and distilled water and placed in an ultrasonic bath after 10 min of centrifuging and was stored at 8 °C [22].

Characterization

The UV-Vis absorbance spectroscopy was performed using a double beam spectrophotometer (VARIAN 300 Conc model). X-ray diffraction (XRD) analysis was recorded from 20° to 80° with a diffractometer (Philips PW1730) using Cu $K_ς$ radiation (λK_a = 1.54 Å) with an accelerating voltage of 40 KV at a scanning rate of 1°/min and counting time of 0.05 s/step. Dynamic light scattering (DLS) analysis was used for hydrodynamic diameter (D_h) calculation. Zeta potential (ς potential) analysis was used to determine colloid stability. The size and morphology of the nanoparticles were evaluated by field-emission scanning electron microscope (FE-SEM, TESCAN MIRA3) at 100 KV of accelerating voltage. Moreover, the confirmation of the particle size and

morphology was also carried out by atomic force microscopy (AFM) (Entegra AFMnt-Mdt Instruments). Fourier transform infrared spectroscopy (FTIR) (NEXUS 8710) analysis was used to identify the functional groups of the samples at wavelengths between 400-4000 cm^{-1} with a resolution of 4 cm^{-1}. The magnetic properties of the synthesized nanoparticles were examined using a vibrating magnetometer (LBKFB of Kashan Desert Magnet Company) with a 1.5 Tesla field of application and a dynamic range of 0.500005 emu.

In Vitro Cytotoxicity Aassay

Cell culture. The MCF-7 cell line (breast adenocarcinoma) and HEK293 cell line (Human embryonic kidney) was provided from Pasteur Institute of Iran. The cells were cultured in RPMI 1640 and DMEM medium respectively containing 10% Fetal Bovine Serum (FBS) and 1% Penicillin-Streptomycin, at 37 °C in a humidified atmosphere with 5% CO_2.

MTT Assay

The MTT assay evaluated the cytotoxic effects of IONPs on MCF-7 and HEK293 cell lines. The cells were seeded into 96-well plates (1×10^4 cells/well) and incubated for 24 h. Then, different concentrations of IONPs (3.125, 6.25, 12.5, 25, 50, 100 µg ml^{-1}) were added to the wells separately, and the plates were incubated for 24, 48 and 72 h. Following the incubation times, 100 µl of MTT (3-(4,5-dimethylthiazol-2-yl)-2,5-diphenyltetrazolium Bromide) (Sigma, Germany) solution (0.5 mg ml^{-1} in PBS) was added to each well of a 96-well plate and the cells were exposed to 37 °C and 5% CO_2. All experiments were carried out in triplicate. Optical absorbance was determined using an ELISA reader at 570 nm wavelength. The results were reported as the cell viability percentage and IC_{50} values (half-maximal inhibitory concentration). The cell viability was computed using the following formula:

$$\%\text{Cell viability} = \frac{\text{absorption of treated cell lines}}{\text{absorption of control cell lines}} \times 100 \quad (2)$$

The cell survival value was compared using One-way ANOVA with a $P \leq 0.05$ considered statistically significant.

RESULTS AND DISCUSSION

Iron Oxide Nanoparticle Biosynthesis

The IONPs was synthesised using *Zhumeria majdae* extract. The immediate color change of the mixture from yellow to dark brown indicates the reduction of ferric hydroxide to Ferric oxide (Fig. 2). The possible chemical reaction for the synthesis of IONPs is shown in Eqs. (1), (2). The functional hydroxyl groups of biomolecules with has the efficiency of reducing the Fe^{3+} ions from $FeCl_3$ precursor. IONPs are formed due to the oxidation of the metal core in the form of a core-shell-core structure [23]. In the process of forming IONPs, there are several phases and the colors of the products are different from each other. For example, magnetite (Fe_3O_4) has a black color, maghemite (γ-Fe_2O_3) has light brown colors, and hematite (α-$Fe_2O_{3)}$ has red colors [24].

$$\textit{Zhumeria majdae}\text{ leaf extract} + FeCl_3 + H_20 \xrightarrow{\text{Stirring}} \textit{Zhumeria majdae}/Fe^{+3} \quad (1)$$

$$\textit{Zhumeria majdae}/Fe^{+3} + 8OH^- \xrightarrow{\text{Stirring}} \textit{Zhumeria majdae}/Fe_3O_4\downarrow + 4H_2O \quad (2)$$

Characterization of the Synthesized Iron Oxide Nanoparticle

The optical absorption properties of magnetite

Fig. 2. Dry leaves zhumeria majdae (an aromatic Herb).

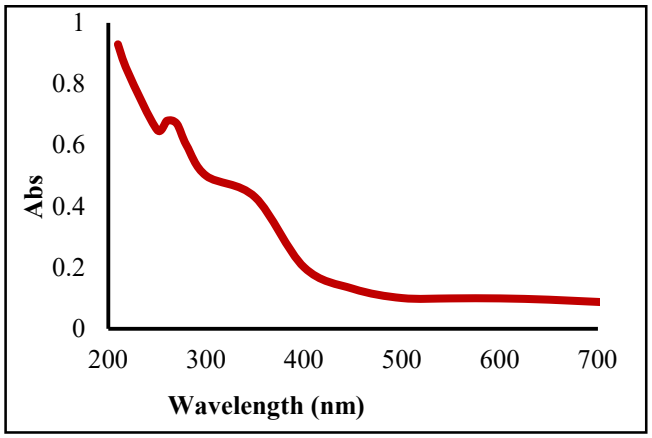

Fig. 3. UV-Vis spectra of Iron nanoparticles produced by Zhumeria majdae metanolic extract. The wavelength was scanned from 200 to 700 nm and the spectra obtained two peaks at 270 nm and 380 nm. No adsorption peak is observed in the range of 400-800 nm.

nanoparticles were determined using UV-Vis Spectrophotometer that were detected two absorption peaks at 270 and 380 nm (Fig. 3). No adsorption peak was observed from 400 to 800 nm. Magnetic nanoparticles show the absorption spectrum in the 330-450 nm region due to their absorption and scattering properties [25]. The absorption spectrum in the region of 270 nm indicate the presence of polyphenols in the plant extractand peak at 380nm is Related to the formation of magnetic nanoparticles. These findings are approved with other studies. The hydrodynamics diameter of nanoparticles were evaluated by DLS method. The hydrodynamic size of IONPs and PEGylated-IONPs was about 34.6 nm and 50.3 respectively. The narrow size distribution of nanoparticles indicates that the plant extract reduce the particle size (Fig. 4A-B). The Zeta potential of IONPs and PEGylated-IONPs was about -29.4 and -38 mV

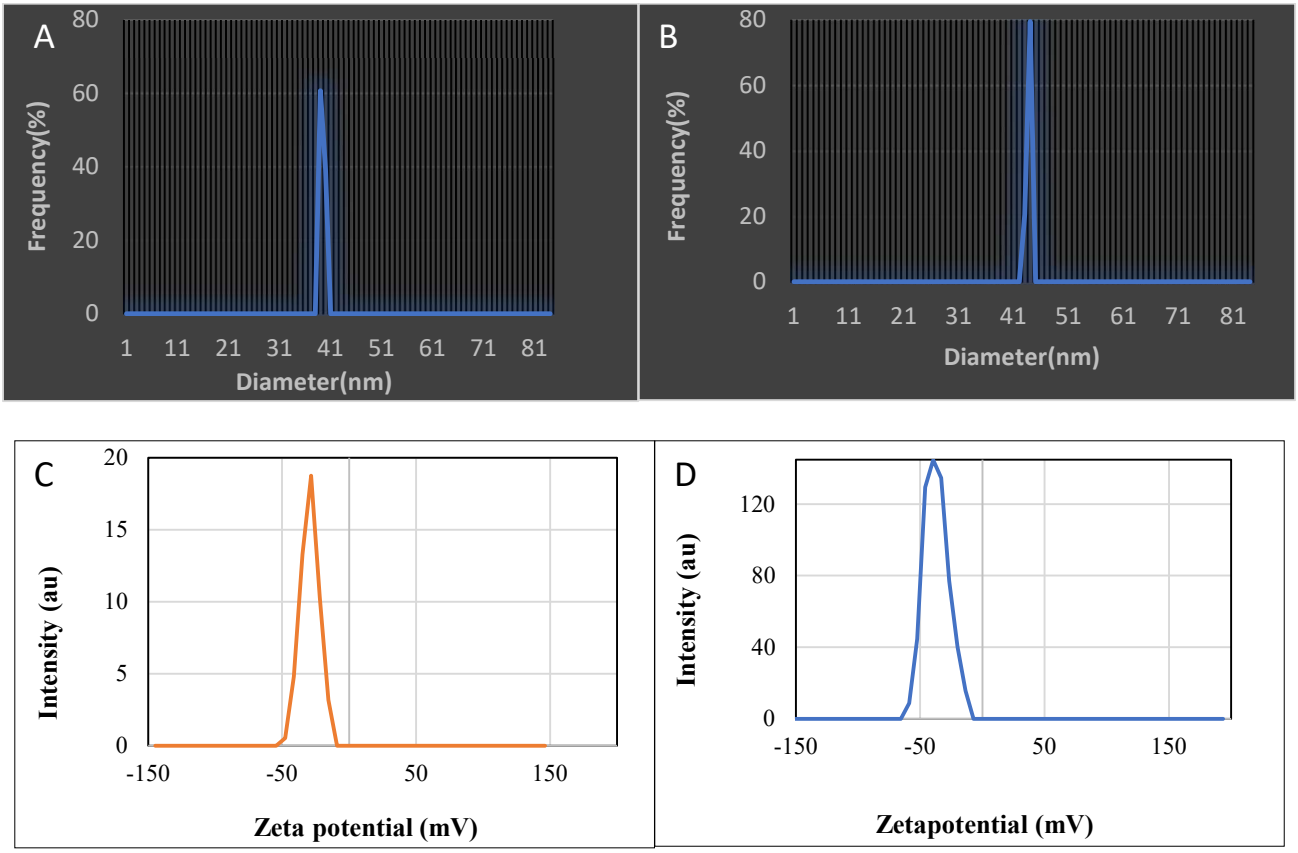

Fig. 4. The hydrodynamic size of IONPs (A) and PEGylated-IONPs (B). Zeta potential values of IONPS (C), PEGylated-IONPs (D). The size of the particles is in the range of nanometers and they have good stability.

respectively (Fig. 4C-D). Carboxyl groups of polyethylene glycol on the surface of IONPs provides more stability through steric repulsion [26]. However, nanoparticles are strongly charged in colloidal systems with zeta potential higher than 30 mV. Therefore, our synthetic nanoparticles have good stability with negative surface charge. SEM and AFM were used to check the size and morphology of nanoparticles. The average size of the synthesized IONPs and PEGylated-IONPs was measuredusing Image J software 15.5 and 12.3 nm respectively (Fig. 5A-B).

The nanoparticles were uniform, relatively polydisperse and spherical in shape with agglomeration in some places. The nature of nanoparticles in aggregates indicates strong intermolecular forces, especially H-bonding between hydroxyl groups and other functional groups present in the structure of bioactive molecules extracted from *Zhumeria majdae* [27]. Pegylated-IONPs were less polydispersity compared to uncoated IONPs. This is because PEG can modify the surface of nanoparticles and reduce their size [28]. Based on data analysis, the DLS diameters were significantly

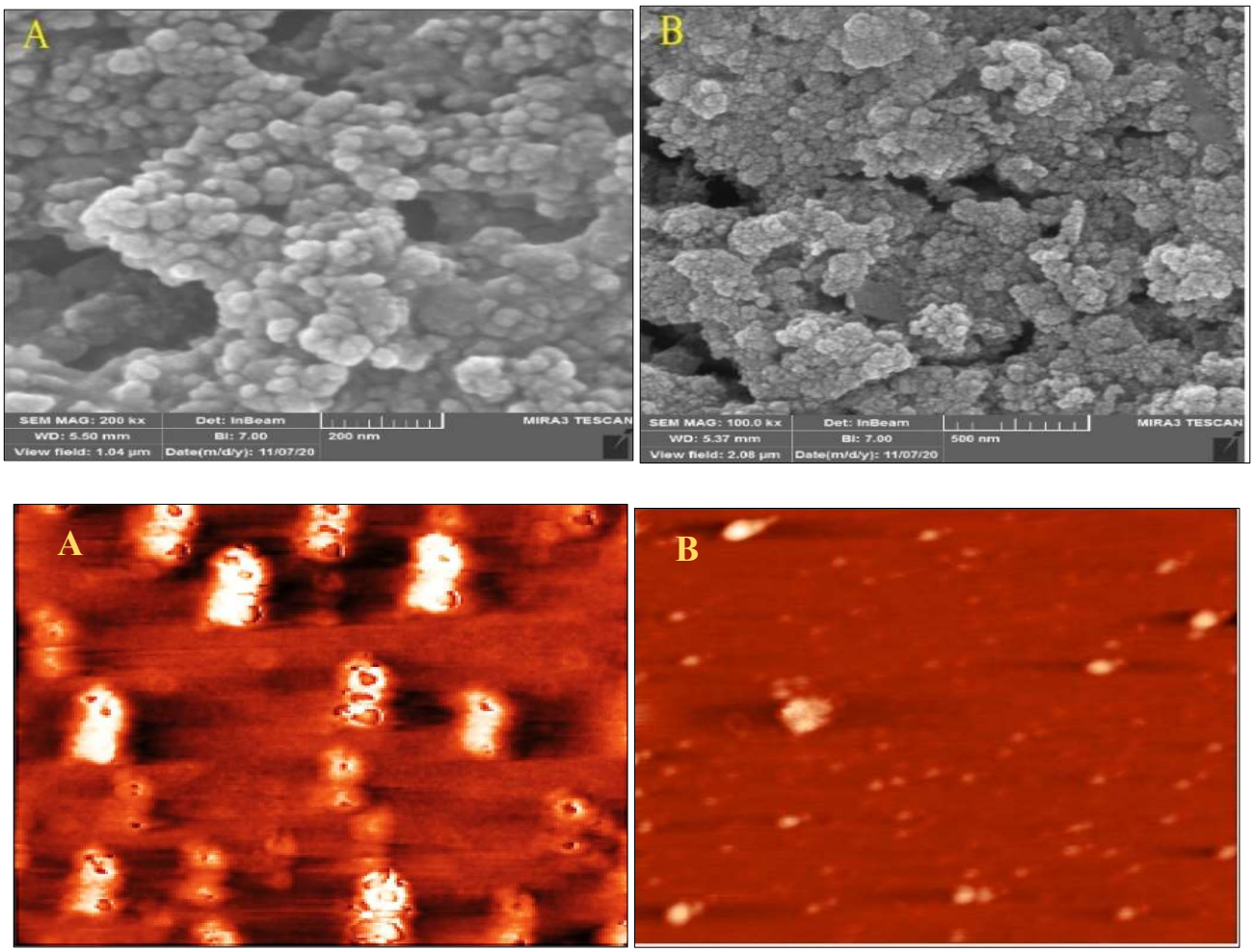

Fig. 5. FE-SEM image of IONPs (A) and PEGylated- IONPs (B) synthesized using Zhumeria majdae extract. The nanoparticles are uniform, relatively polydisperse and spherical in shape with agglomeration in some places. The average size of the synthesized IONPs and PEGylated-IONPs was calculated 15.5 and 12.3 nm respectively. and atomic force microscopic image of IONPS (C) and PEGylated-IONPs (D). AFM topographic two dimensional images indicated the physically polydispersed compounds. AFM images confirm the results of SEM.

larger than SEM and XRD sizes. The differences could be due to the fact that SEM estimates the physical size while DLS calculates the hydrodynamic size of the particles [29]. AFM analysis evaluates topographic features of the surface of nanoparticles (Fig. 5C-D). The two dimensional view clearly shows an asymmetric distribution of particles per unit area. This behavior of nanoparticles is due to the effectiveness of bioactive molecules extracted from *Zhumeria majdae* such as terpenoids and polyphenols [30]. Nanoparticles are oriented in one direction due to their magnetic properties. The AFM roughness parameters for IONPs and pegylated-IONPs were calculated using Nova software 0.198, 0.4 nm respectively. Due to the presence of PEG polymer on the surface of nanoparticles, the affinity increases. AFM images confirm that the size of nanoparticles is in the nanometer range. These findings agree with the results of SEM. Figure 6 shows the X-ray diffraction spectrum of the synthesized nanoparticles using the *Zhumeria majdae* extract. The spectrum was recorded with a counting time of 0.05 s/step and 2theta/theta range of 20-80 degrees at an X-ray wavelength of 1.54 nm.

The peaks observed in XRD analysis revealed the spinal structured magnetite and exhibiting peaks at 2 theta value of 30.47, 35.74, 43.49, 53.90, 57.20, 62.94, 74.50, which corresponds to diffraction planes of (220), (311), (400), (422), (511), (440) and (533), respectively. The formation of IONPs index with ICDD card no:00- 25-1402. The analysis also revealed that the synthesized nanoparticles have a crystalline structure and are pure. XRD results support those reported previously [31]. The average grain size was 26.5 nm, which was calculated from the FWHM of the XRD peaks using the Debye-Scherrer equation (Eq. (3). Where, λ is the wavelength of the X-rays (0.1541 Å), 0.90 is a dimension constant value known as shape factor, ß is the FWHM and θ is the most intense peak's Bragg angle [32]. By comparing the SEM and XRD values, conclude that there are single-crystal nanoparticles and particle size and crystallite size are the same.

$$D = \frac{0.9\lambda}{\beta\cos\theta} \quad (3)$$

The FTIR spectra of *Zhumeria majdae* extract, IONPs, and Pegylated-IONPs are shown in Fig. 7. FT-IR analysis of

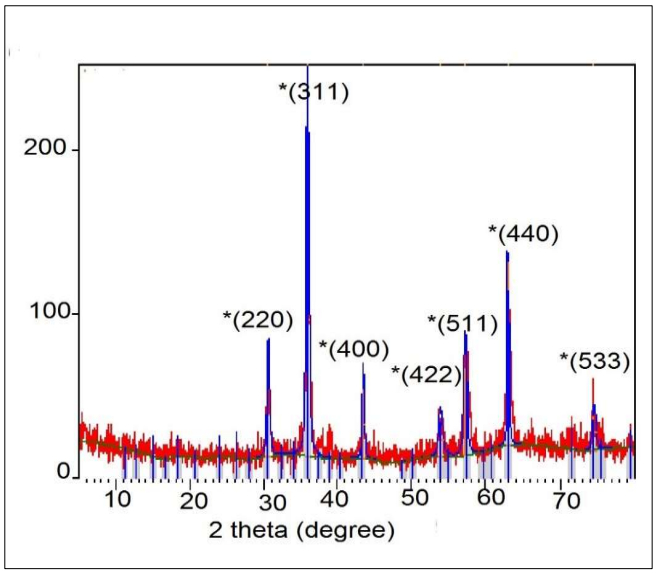

Fig. 6. X-ray diffraction (XRD) pattern of IONPs synthesized using Zhumeria majdae extract. The XRD pattern showing 2θ = 30.47, 35.74, 43.49, 53.90, 57.20, 62.94, 74.50. The average size of the nanoparticles synthesized were determined from the FWHM of the XRD peaks 26.5 nm.

Zhumeria majdae extract indicates that absorption bands are detected in the following wavelength ranges: 3433 cm^{-1}, 2923 cm^{-1}, 1928 cm^{-1}, 1461 cm^{-1}, 1261 cm^{-1},1016 cm^{-1}, and 691 cm^{-1} (Fig. 7A). The peak at 3433cm^{-1} corresponds to the O-H stretching frequency out of the plane bending mode of the phenolic group. This band was shifted to 3432 cm^{-1} in nanoparticles most likely because of phytochemicals binding and the presence of water molecules on the surface of the particles which allows it to bind to the PEG-4000 polymer. the absorption peaks at 2923 cm^{-1} and 1928 cm^{-1} belong to the stretching vibration of the C-H bonds of aliphatic and aromatic functional groups, and C-C alkene group in terpenes respectively [33]. Those bands centered at 1461 cm^{-1} relate to a bend in the C-O-H of the hydroxyl group of *Zhumeria majdae* extract. C-O stretching in polyols causes the bands at 1261 cm^{-1}. These phytochemicals which act as reducing and capping agents for the nanoparticles, lead to the colour change from yellowish to dark brown. The IONPs showed dominant absorption peaks associated with Fe-O vibrations at 456 cm^{-1} (Fig. 7B). This peak of in the absorption spectrum indicates that the Magnetite phase has been formed in the

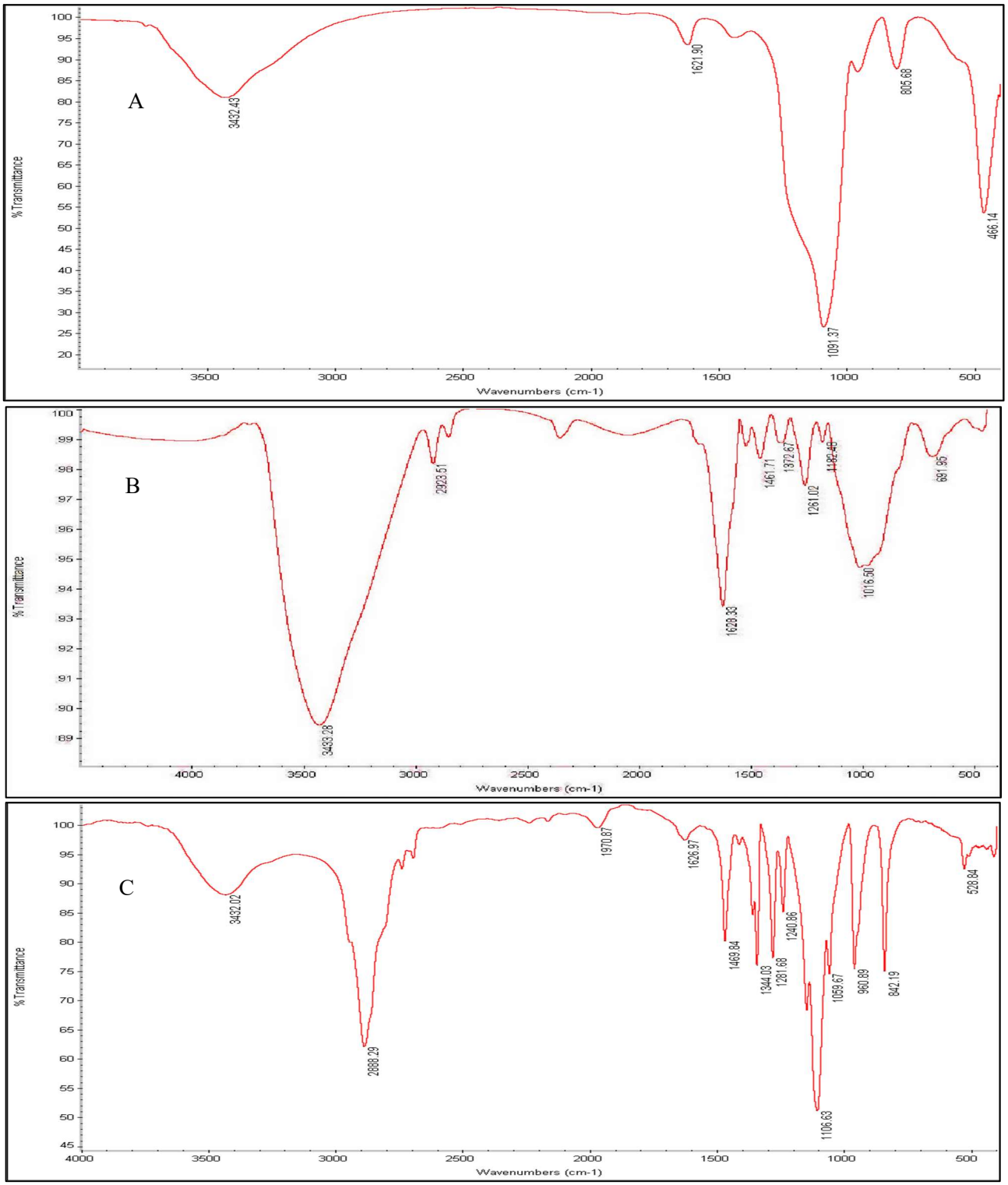

Fig. 7. FT-IR spectrum of Zhumeria majdae leaf extract (A), IONPs (B) and Pegylated IONPs (C). FT-IR spectroscopy measurements were recorded by using a Perking Elmer, spectrometer with a scan range from 400-4000 cm^{-1} with resolution of 4 cm^{-1}. FTIR spectra of the prepared IONPs, indicating presence of organic compounds from Zhumeria majdae.

synthesized nanoparticles. A similar peak was observed in the Pegylated-IONPs spectra at 528 cm^{-1} (Fig. 7C). Magnetite absorbance band is detected at 400 and 570 cm^{-1}. The Maghemite absorbance band is observed between 620 and 660 cm^{-1} [24]. Therefore, Fe-O stretches at the 456 cm^{-1} belongs to the magnetite nanoparticles. A stretch of C–O of about 1106 cm^{-1} was observed in Pegylated-IONPs. However, this peak was not observed in the uncoated nanoparticle spectrum, revealing the presence of PEG residue in the final product. These results clearly show the surface modification of nanoparticles with PEG-4000 [34]. Overall, the detected absorbance bands is concurrent with UV-Vis spectroscopy analysis. Figure 8 shows the magnetic field versus magnetic moment curve for IONPs at room temperature. The IONPs showed no significant hysteresis in their magnetization curve and was completely reversible. The maximum saturation magnetization (Ms) gain is 1.13 emu/g with zero coercivity in the M-H plot. The low of saturation magnetization at high fields is due to the small particle size and the large surface area [35], therefore it can react to strong external magnetic field with superparamagnetic behavior because there was no residual magnetism before and after removal of external magnetic field [36]. Besides, low saturation magnetization (Ms) of nanoparticles indicates successful implant of *Zhumeria majdae* extract on the surface of the nanoparticles. These findings indicate that our biosynthesized nanoparticles can be used for magnetic drug targeting and other biomedical applications especially hyperthermia.

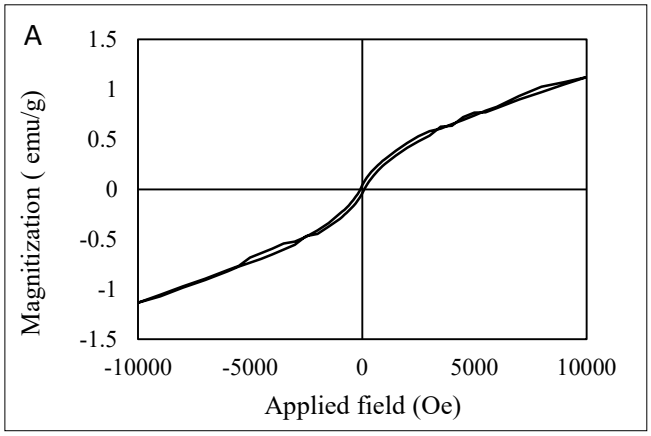

Fig. 8. Magnetization curve of the biosynthesized IONPs. The data is presented in terms of Ms, mass magnetization (emu/g), *versus* H, applied magnetic field (Oe). magnetization value of the synthesized IONPs was measured to be 1.13 memu/g. The image shows that nanoparticles do not have hysteresis loop and are super paramagnetic in nature.

In Vitro Cytotoxicity Study

The cell viability of IONPs was analyzed by using MTT assay (Fig. 9). Incubation of the mcf-7 and HEK293 cell lines at different concentrations (3.125 µg ml^{-1}, 6.25 µg ml^{-1}, 12.5 µg ml^{-1}, 25 µg ml^{-1}, 50 µg ml^{-1}, and 100 µg ml^{-1}) of nanoparticles after 24, 48 and 72 h showed a dose-dependent decrease in cell viability compared to control proup. The cytotoxicity effect of biosynthesized IONPs against mcf-7 cell lines revealed that nanoparticles are capable of inhibiting the growth of cancer cells as the concentrations of nanoparticles increases. The result obtained from the *in vitro* cytotoxicity evaluation of various concentrations of IONPs synthesized using Z. majdae against MCF-7 cell lines revealed toxicity efficacy at concentrations of 50 µg ml^{-1} and

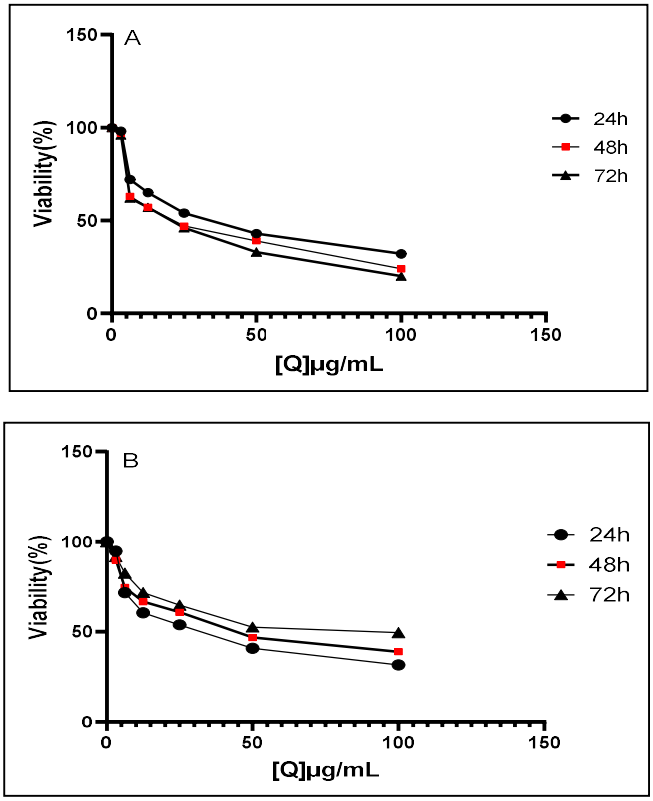

Fig. 9. Concentration-dependent cell viability of IONPs on MCF-7 cell lines (A) and HEK293 cell lines (B). Percentage cell viability after MCF-7 (A) and HEK293 (B) treatment with the various concentrations of nanoparticless.

above. According to the diagram, nanoparticles did not show any toxic effects on HEK293 cells and are completely safe.

CONCLUSION

By green chemistry, we synthesized IONPs with the aim of application in targeted drug delivery for breast cancer treatment. As *Zhumeria majdae* has not previously been used to synthesize IONPs, this study presents a novel green synthesis of IONPs using Hormozgan-grown *Zhumeria majdae*. The first time trial of nanoparticle formulation was confirmed by UV-Vis, DLS. Zeta potential, XRD, SEM, AFM, VSM and FTIR techniques. The adopted green chemistry approach synthesized IONPs in nano-scale size, uniform spherical shape. Results revealed that *Zhumeria majdae* leaf extract has potential bioactive molecules that can be employed for Fe_3O_4 nanoparticles fabrication. The drug delivery system fabricated by us providing more targeted drug accumulation in the breast adenocarcinoma cells owing to their small size and magnetic nature. Further, the *Zhumeria majdae*/IONPs can be conjogated with anticancer agents to increase efficacy and induce apoptosis in the breast adenocarcinoma cells.

ACNOWLEDGMENTS

This research has been supported by the Research Council of Kharazmi University and the Science and Research Branch of Islamic Azad University. We have gratefully acknowledged their support.

REFERENCES

[1] J. Sandhya, S. Kalaiselvam, Mater. Res. Express. 158 (2020) 338.

[2] K. Tharani, L.C. Nehru, International J. Adv. Res. Phys. Sci. 2 (2015) 47.

[3] H.F. Kiwumulo, H. Muwonge, C. Ibingira, M. Lubwama, J.B. Kirabira, R.T. Sekitoleko, BMC Research Notes. 15 (2022).

[4] J. Singh, T. Dutta, K.-H. Kim, M. Rawat, P. Samddar, P. Kumar, J. Nanobiotechnol. 16 (2018).

[5] C, M. G, In International Journal of Agriculture Innovations and Research. 6 (2017).

[6] S.A. Akintelu, A.K. Oyebamiji, S.C. Olugbeko, A.S. Folorunso, In Ecletica Quimica Atlantis Livros Ltda. 46 (2021) 17.

[7] S.P. Patil, R.Y. Chaudhari, M.S. Nemade, In Talanta Open. Elsevier B.V. 5 (2022) 100083.

[8] F. Namjoyan, A. Jahangiri, M.E. Azemi, H. Mousavi, Pharmaceutical Sci. 22 (2016) 81.

[9] G. Azimia, J. Asgarpanaha, Brazilian Journal of Biology. 81 (2021) 881.

[10] L. Baghazadeh -Daryaii1, D. Samsampour, A. Bagheri, M. Askari-Seyahooei, M. Raam, International Journal of Horticultural Science and Technology. 7 (2020).

[11] A. Karami, F. Tashani, A. Tahmasebi, F. Maggi, Horticulturae. 7 (2021).

[12]A. Zangeneh, M.M. Zangeneh, R. Moradi, Appl. Oganometallic Chem. 34 (2020).

[13] H. Tolouietabar1, A.A. Hatamnia1, R. Sahraei, E. Soheyli, Biologically green synthesis of high-quality silver nanoparticles using scrophularia striata boiss plant extract and verifying their antibacterial activities. 10 (2020) 44.

[14] V. Abdi, I. Sourinejad, M. Yousefzadi, Z. Ghasemi, Mangrove-mediated synthesis of silver nanoparticles using native Avicennia marina plant extract from southern Iran Chemical Engineering Communications. 205 (2018) 1069.

[15] S. Nasiri, S. Nasiri, Biosynthesis of Silver Nanoparticles Using Carum carvi Extract and its Inhibitory Effect on Growth of Candida albicans. 4 (2016) e37504.

[16] M. Kazemi, Environmental Resources Research. 9 (2021).

[17] Z. Mohammadi-Ziveha, S.A. Mirhosseini, H. Mahmoodzadeh, Iran. J. Pharmaceut. Res. 19 (2020) 169.

[18] Y.S. Hajizadeh, N. Harzandi, E. Babapour, M. Yazdanian, Advances in Materials Science and Engineering. (2022).

[19] S. Salehi, S.A. Sadat Shandiz, F. Ghanbar, M.R. Darvish, M.S. Ardestani, A. Mirzaie, M. Jafari, International Journal of Nanomedicine. 11 (2016) 1835.

[20] B. Mousavi, F. Tafvizi, S.Z. Bostanabad, Artificial Cells, Nanomedicine, and Biotechnology. 46 (2018) 499.

[21]A. Gholami, R. Khosravi, A. Khosravi, Data in Brief.

21 (2018) 779.

[22] S. Prabhu, S. Mutalik, S. Rai, N. Udupa, B.S.S. Rao, Journal of Nanoparticle Research.17 (2015).

[23] N.V. Srikanth Vallabani, Sanjay Singh. Recent advances and future prospects of iron oxide nanoparticles in biomedicine and diagnostics. 3 Biotech. 8 (2018).

[24] D. Aksu Demirezen, Y.S. Yıldız, S. Yılmaz, D. Demirezen Yılmaz, J Biosci. Bioengin. 127 (2019)241.

[25] S. Amutha, S. Sridhar, Journal of Innovations in Pharmaceutical and Biological Sciences. 5 (2018) 22.

[26] S. Satpathy, A. Patra, B. Ahirwar, M.D. Hussain, Nanomedicine and Biotechnology. 46 (2018) 71.

[27] I. Bibi, N. Nazar, S. Ata, M. Sultan, A. Ali, A. Abbas, K. Jilani, S. Kamal, F.M. Sarim, M.I. Khan, F. Jalal, M. Iqbal, J. Mater. Res. Technol. 8 (2019) 6115.

[28] J.S. Suk, Q. Xu, N. Kim, J. Hanes, L.M. Ensign, PEGylation as a strategy for improving nanoparticle-based drug and gene delivery. 99 (2016) 28.

[29] H. Erjaee, H. Rajaian, S. Nazifi, Advances in Natural Sciences: Nanoscience and Nanotechnology. 8 (2017) 025004.

[30] AO. Kalu, EC. Egwim, AA. Jigam, H.L. Muhammed, Nano Express. 3 (2022) 045004.

[31] S. Ahmadi, M. Fazilati, H. Nazem, BioMed. Research International. 9 (2021) 1.

[32] N. Basavegowda, K. Bahadur Somai Magar, K. Mishra, Y. Rok Lee, New J. Chem. 38 (2014).

[33] M. Rahimivand, F. Tafvizi, H. Noorbazargan, Synthesis and characterization of alginate nanocarrier encapsulating Artemisia ciniformis extract and evaluation of the cytotoxicity and apoptosis induction in AGS cell line. 158 (2020).

[34] E. Suharyadi, G. Antarnusa, Materials Research Express. 7 (2020) 056103.

[35] L. Cabrera, S. Gutierrez, N. Menendez, M.P. Morales, P. Herrasti, Electrochim. Acta 53 (2008) 3436.

[36] A.V. Samrot, C.S. Sahithya, A.J. Selvarani, S.K. Purayil, P. Ponnaiah, Current Research in Green and Sustainable Chemistry. 4 (2021) 100042.